Materials Research Proceedings **9** (2018) 32-37 doi: http://dx.doi.org/10.21741/9781644900017-7

Thermomechanical and Magnetic Properties of Fe-Ni-Co-Al-Ta-B Superelastic Alloy

Victor V. Koledov[1,a], Elvina T. Dilmieva[1,b], Vladimir S. Kalashnikov[1,c], Alexander P. Kamantsev[1,d*], Alexey V. Mashirov[1,e], Svetlana V. von Gratowski[1], Vladimir G. Shavrov[1], Alexey V. Koshelev[2], Vedamanickam Sampath[3], Irek I. Musabirov[4], Rostislav M. Grechishkin[5]

[1]Kotelnikov Institute of Radio-engineering and Electronics of RAS, 11-7 Mokhovaya Str., Moscow 125009, Russia

[2]Lomonosov Moscow State University, 1 Leninskie Gory, Moscow 119991, Russia

[3]Indian Institute of Technology Madras, Chennai 600036, India

[4]Institute for Metals Superplasticity Problems of RAS, 39 Stepana Halturina Str., Ufa 450001, Russia

[5]Tver State University, 33 Zhelyabova Str., Tver 170100, Russia

[a]victor_koledov@mail.ru, [b]kelvit@mail.ru, [c]vladimir.kalashnikovS@gmail.com, [d]kaman4@gmail.com, [e]a.v.mashirov@mail.ru

*corresponding author

Keywords: Phase Transition, Shape Memory Effect, Superelasticity, Strain Glass, Spin Glass, Fe-Ni-Co-Al-Ta-B, Superstructures

Abstract. The ingot of $Fe_{40.71}Ni_{27.33}Co_{17.13}Al_{12.05}Ta_{2.73}B_{0.05}$ alloy was produced by arc melting technique followed by heat treatment. The alloy ingot was cut by electro-discharge machining and was further subjected to rolling. The microstructure of surface, thermomechanical and magnetic properties were studied. The alloy exhibits superelasticity at temperature lower than 330 K. The hysteretic behavior of magnetization was observed. These properties can be explained by combination of states of the spin- and strain-glasses.

Introduction

Ferromagnetic iron-containing Heusler alloys exhibiting shape memory effect (SME), such as Ni-Mn-Ga-Fe demonstrate reversible deformations of up to several % due to thermoelastic martensitic transition induced by magnetic field [1]. The iron-based, high-strength Fe-Ni-Co-(Al-Ta-B) alloy with superplasticity and reversible deformations of more than 13 % with a tensile strength above 1 GPa is discussed in [2]. The tensile strength of this alloy is almost twice that for the highest stress for superelastic deformation in Ni-Ti alloys. In addition, this iron-containing alloy also shows high damping and reversibility of magnetization during loading and unloading processes. More recently, other iron-containing alloys exhibiting superelasticity have attracted attention [3-7]. The investigations of a nanostructured FeMnSi shape memory alloy produced via severe plastic deformation is done in [8]. The family of Fe-Ni-Co-(Al-Ta-B) alloys demonstrates unique physical properties: a wide temperature hysteresis of superelasticity, a change in magnetization over a larger range, and electrical resistance due to load, accompanied by high pseudoplasticity. In view of these properties, these iron-containing superelastic alloys are expected to be used for a wide range of practical applications, such as damping and functional materials. Significant interest in these alloys is caused by the quest for inexpensive structural materials for the fabrication of structures that are resistant to earthquakes, such as nuclear power plants, high-rise buildings, bridges and industrial facilities.

Materials Research Proceedings **9** (2018) 32-37 doi: http://dx.doi.org/10.21741/9781644900017-7

This paper presents the results of the experimental study of new $Fe_{40.71}Ni_{27.33}Co_{17.13}Al_{12.05}Ta_{2.73}B_{0.05}$ (FNCATB) alloy: the microstructure of surface, the occurrence of structural phase transitions (PT) due to temperature, mechanical stress as well as magnetic field in wide temperature range 4–400 K.

Samples and Microstructure

The FNCATB alloy ingot was made by arc melting in an argon atmosphere with subsequent heat treatment. The ingot was annealed for 24 hours at temperature of 1493 K, followed by a thermal aging of 72 hours at 873 K. Then the plates were cut by the electroerosive method in the form of plates, which were subsequently thinned by cold rolling.

The homogeneity of the FNCATB alloy was investigated by the EDX method – the chemical composition of the sample was studied at 8 points. Table 1 presents the maximum and minimum values of the weight percent of the chemical elements fixed in the alloy in the volume under study. The obtained alloy has a satisfactory homogeneity and the obtained chemical composition is close to the one set within the error of measurement. The EDX method has an error of about 0.3–0.5 % by weight, therefore it does not allow to fix the presence of boron in the sample.

Table 1. The composition of the sample of the FNCATB alloy [at.%].

	Al	Fe	Co	Ni	Ta	B
Max	6.98	40.19	17.53	28.46	6.61	-
Min	6.26	38.80	17.10	27.62	7.47	-

Studies of the microstructure of the sample using a scanning electron microscope revealed the multiphase nature of the FNCATB alloy at room temperature. Also, it can be seen from Fig. 1(a), that the sample has a dendritic structure, possibly associated with the heat sink process in the manufacture of the sample.

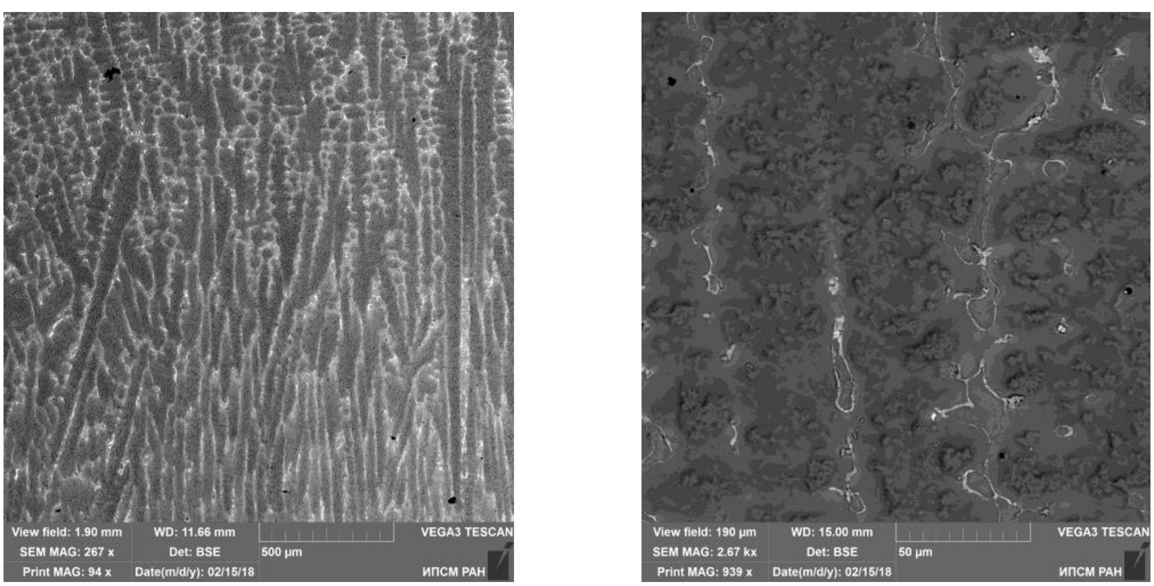

(a) (b)

Figure 1. Photographs of the surface structure of the FNCATB sample taken with a scanning electron microscope: (a) 500 μm and (b) 50 μm scales.

Metallographic studies were carried out by polarization optical microscope. The sample was polished above room temperature at 330 K. Fig. 2 (a) demonstrates the microstructure of the FNCATB alloy at room temperature. The martensitic phase appeared on the surface of the metallographic section after additional thermal cycling (cooling down to K and heating to

Materials Research Proceedings **9** (2018) 32-37 doi: http://dx.doi.org/10.21741/9781644900017-7

300 K), which also proves the presence of the structural PT of the 1-st order in the FNCATB alloy (Fig. 2(b)). The additional electropolishing (Fig. 2(c)-(f)) made it possible to reveal the nature of the precipitates of the phases of the alloy.

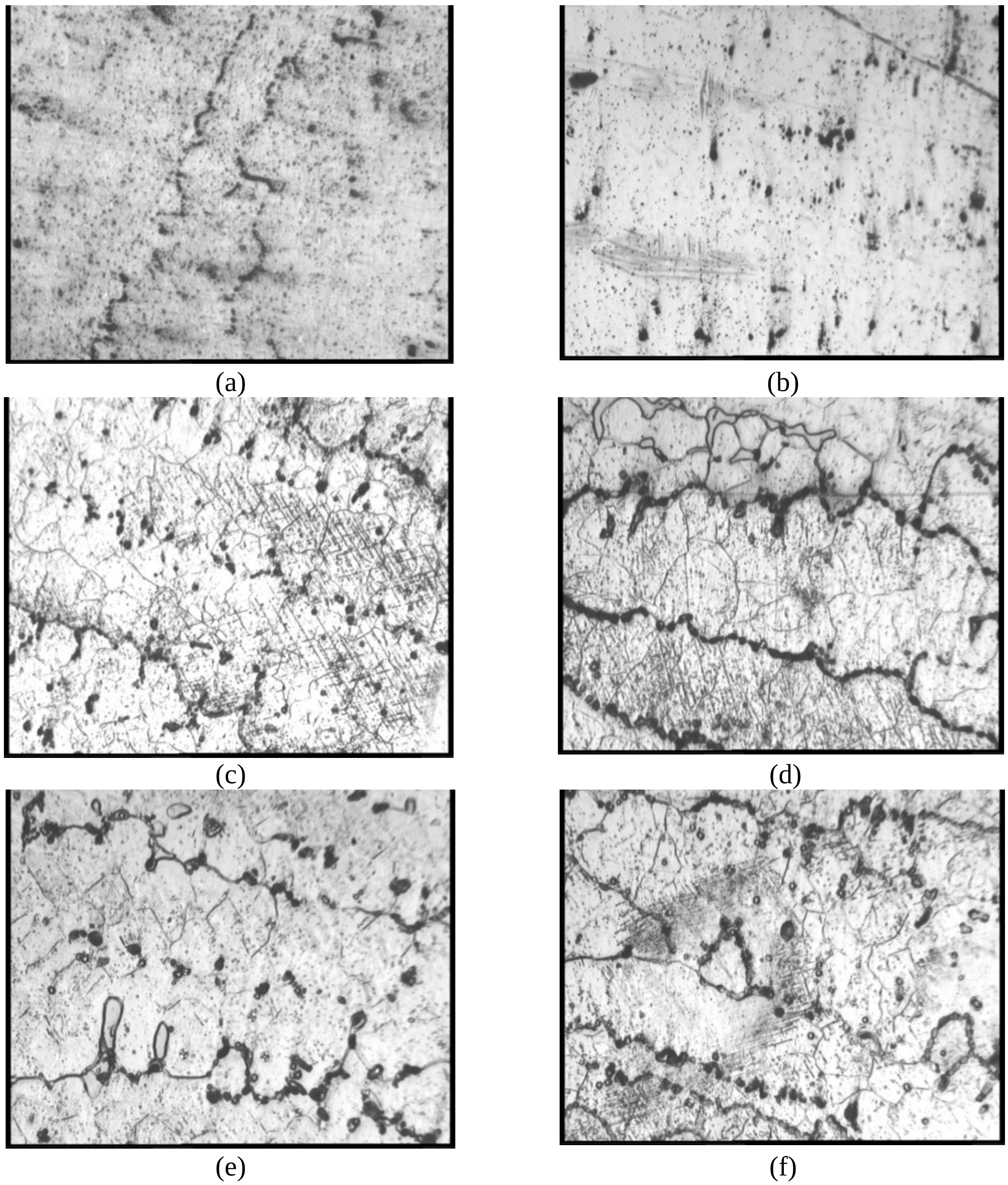

Figure 2. The microstructure of the FNCATB (a) alloy at room temperature, (b) after additional cooling downto 77 K and heating to 300 K, (c)–(f) after electropolishing at room temperature.

Experimental Results

The Fig. 3 shows the temperature dependences of the magnetization of the FNCATB sample obtained by using the ZFC-FC-FH protocol in magnetic field with induction of 3 T and in low field of 50 Oe (in the inset). There is an anomaly of the behavior of the magnetization curve like hysteresis in low field near the room temperature, which presupposes the presence of the 1-st order PT in the alloy. The magnetization dependence typical for ferromagnetic materials was

Materials Research Proceedings **9** (2018) 32-37 doi: http://dx.doi.org/10.21741/9781644900017-7

observed in the high field during the heating, hysteresis behavior was observed during the cooling. These results can be explained by the combination of states of the spin and deformation glass in the FNCATB alloy in wide temperature range of 100–400 K.

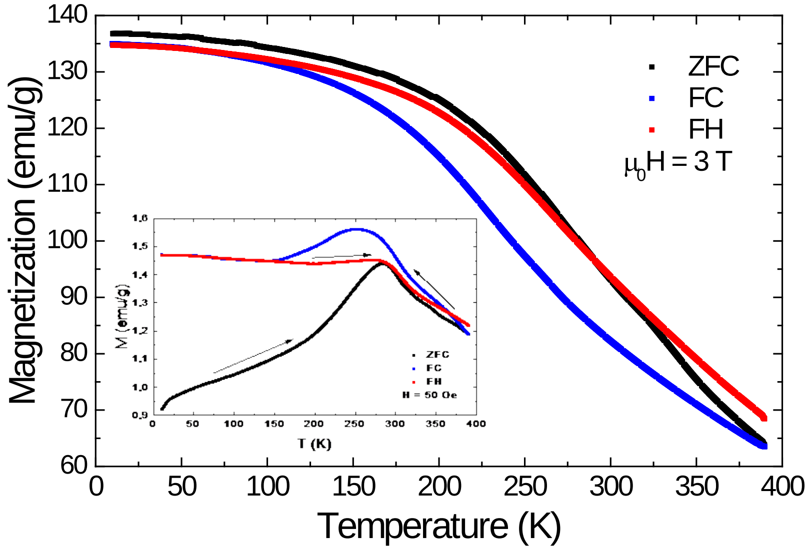

Figure 3. Temperature dependence of magnetization of the FNCATB alloy in magnetic field with induction of 3 T. In the inset: the temperature dependence of magnetization of the FNCATB alloy in magnetic field of 50 Oe.

To study the functional properties of alloys with giant effect of superelasticity an experimental setup was used to determine the thermomechanical properties of alloys in the temperature range 140–570 K, mechanical stresses up to 2000 MPa and deformations up to 20 %. The principle of the installation is based on the method of three-point bending of the sample at variable temperature and constant load. The installation was tested on samples of the known alloy $Ni_{49.8}Ti_{50.2}$, which confirmed the reliability of the results obtained on it [9].

The Fig. 4 shows the results of the study of the temperature dependence of the deformation of the FNCATB sample. The research protocol was as follows. The sample was heated from 140 K to 370 K without load. Then, the stresses of 527 MPa were reached by applying external mechanical force at temperature of 370 K. The sample was cooled to 140 K and then heated to 410 K under load. The deformation versus temperature curve for heating and cooling shows deviation from the linear dependence, which indicates the presence of pseudoplasticity and SME in the sample. The value of the SME is not more than 0.3%. The temperatures of the beginning and the end of the thermoelastic PT are indicated in the Fig. 4.

The Fig. 5 shows the dependence of the strain of the sample upon loading at 368 K. The dependence also reflects the deviation from Hooke's law (from linearity). The curve σ (ε) shows the location of the kink, where a deviation is observed, which corresponds to the stress of the PT under load and is approximately 370 MPa.

The Fig. 6 shows the dependence of the deformation on the load for three loading-unloading cycles at temperature of 298 K. It is noted that as the number of thermocycles increases, the stress at which the PT is observed decreases. On the graphs, when the load is removed, the deformation of the sample after the load is removed is somewhat lower than the deformation of the sample under load. This phenomenon is instrumental in nature and is a feature of the installation on which the test was carried out.

Materials Research Proceedings **9** (2018) 32-37 doi: http://dx.doi.org/10.21741/9781644900017-7

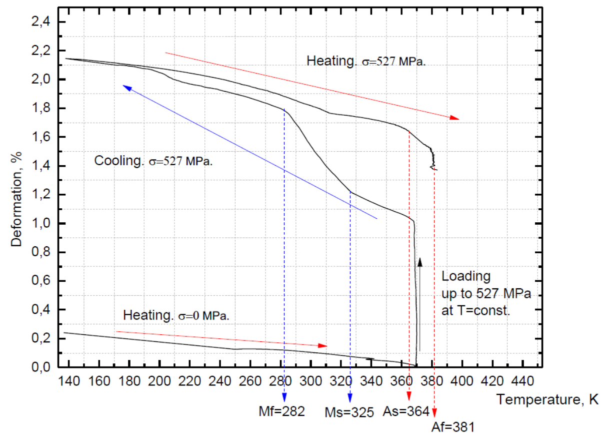

Figure 4. Temperature dependence of the deformation of the FNCATB alloy under different loads.

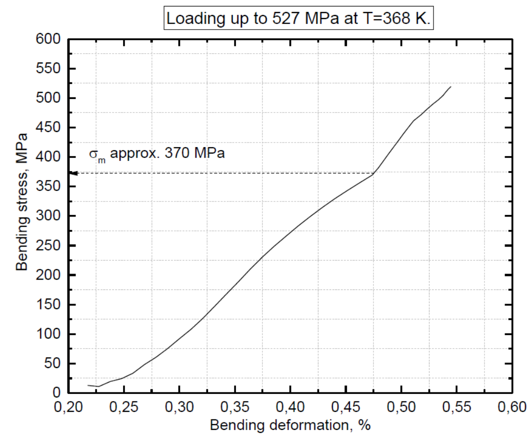

Figure 5. Dependence of the deformation of the FNCATB alloy under loading at 368 K.

The Fig. 7 shows the results of thermocycling the sample under load and without load. The structural PT was observed during the first cycles of heating loading in the FNCATB sample. The load was removed on the third cycle, and the PT was observed before the 7th cycle. Then the PT was absent – the effect of the sample training disappeared or the relaxation of the stresses induced during the first reward cycles occurred.

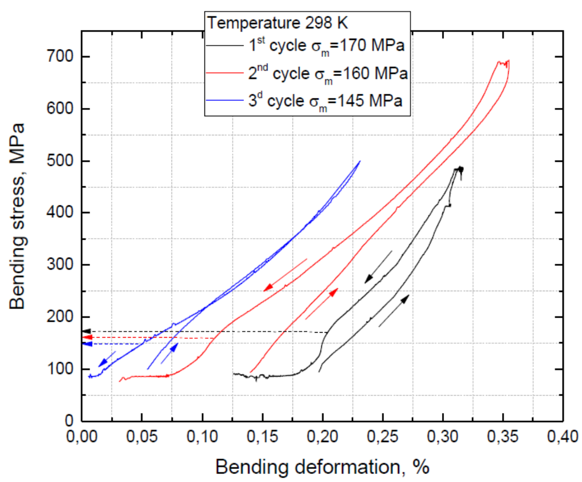

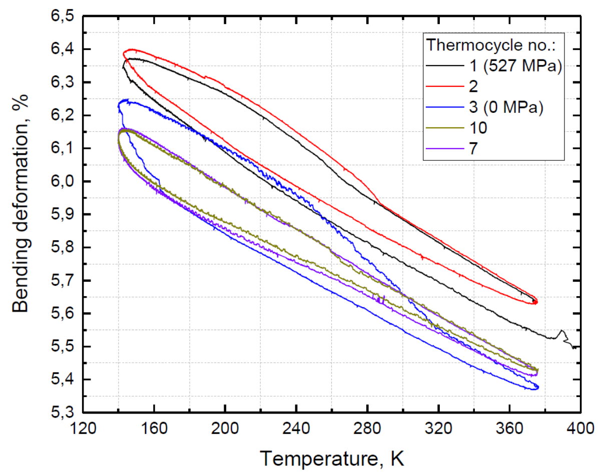

Figure 6. Dependence of strain on load for three loading-unloading cycles of the FNCATB alloy.

Figure 7. Temperature dependence of the deformation of the FNCATB alloy under load and without load up to the 7th thermal cycle.

Conclusions

In this paper we present the results of the study of the $Fe_{40.71}Ni_{27.33}Co_{17.13}Al_{12.05}Ta_{2.73}B_{0.05}$ (FNCATB) alloy, an experimental study of their microstructure, the appearance of a structural PT induced by temperature and mechanical stress, and also by a magnetic field.

1) The ingot of FNCATB alloy was made by the arc melting method followed by homogenizing annealing and ageing, then plates were made by electric cutting and rolling. The initial composition was confirmed by EDX analysis.

2) The microstructure of the alloy surface was studied by optical metallography and scanning electron microscopy. The multiphase of the FNCATB alloy was revealed at room temperature, and a dendritic surface structure was also detected.

3) The typical behavior of magnetization versus temperature dependence at heating is observed, and hysteresis behavior is manifested at cooling in high magnetic field. These results can be explained by the combination of states of the spin- and strain-glass in the FNCATB alloy in wide temperature range 100–400 K.

4) The thermoelastic PT of the 1-st order was detected by the dilatometric method in the temperature range 282–381 K, while the SMA value does not exceed 0.3 % at load of 527 MPa. The effect of superelasticity at temperatures below 330 K in the FNCATB alloy is shown.

Studies of iron-containing alloys with effects of superelasticity should be continued, because a combination of strong superelasticity and high reliability with a relatively low price and manufacturability is of great interest for creating superstructures resistant to extreme loads.

Acknowledgments
The work is supported by RFBR, Grants No. 16-57-45066, 17-07-01524.

References

[1] A.A. Cherechukin et al., Shape memory effect due to magnetic field-induced thermoelastic martensitic transformation in polycrystalline Ni-Mn-Fe-Ga alloy. Phys. Lett. A. 291 (2001) 175. https://doi.org/10.1016/S0375-9601(01)00688-0

[2] Y. Tanaka et al., Ferrous polycrystalline shape-memory alloy showing huge superelasticity, Science. 327 (2010) 1488. https://doi.org/10.1126/science.1183169

[3] S. Bhowmick, S.K. Mishra, FNCATB Superelastic damper for seismic vibration mitigation, J. Intel. Mat. Syst. Str. 27 (2016) 2062. https://doi.org/10.1177/1045389X15620039

[4] T. Omori, K. Ando, M. Okano, X. Xu, Y. Tanaka, I. Ohnuma, K. Ishida, Superelastic effect in polycrystalline ferrous alloys, Science. 333 (2011) 68-71. https://doi.org/10.1126/science.1202232

[5] T. Omori, S. Abe, Y. Tanaka, D.Y. Lee, K. Ishida, R. Kainuma, Thermoelastic martensitic transformation and superelasticity in Fe-Ni-Co-Al-Nb-B polycrystalline alloy, Scripta Mater. 69 (2013) 812-815. https://doi.org/10.1016/j.scriptamat.2013.09.006

[6] D. Lee, T. Omori, R. Kainuma, Ductility enhancement and superelasticity in Fe-Ni-Co-Al-Ti-B polycrystalline alloy, J. Alloy. Compd. 617 (2014) 120-123. https://doi.org/10.1016/j.jallcom.2014.07.136

[7] Y. Tanaka, R. Kainuma, T. Omori, K. Ishida, Alloy Design for Fe-Ni-Co-Al-based Superelastic Alloys, Mater. Today: Proc. 2 (2015) S485-S492. https://doi.org/10.1016/j.matpr.2015.07.333

[8] G. Gurau, C. Gurau, V. Sampath, L.G. Bujoreanu, Investigations of a nanostructured FeMnSi shape memory alloy produced via severe plastic deformation, Int. J. Miner. Metall. Mater. 23 (2016) 1315-1322. https://doi.org/10.1007/s12613-016-1353-6

[9] V.S. Kalashnikov, V.V. Koledov, D.S. Kuchin, A.V. Petrov, V.G. Shavrov. A three-point bending test machine for studying the thermomechanical properties of shape memory alloys, Instrum. Exp. Tech. 61 (2018) 306-312. https://doi.org/10.1134/S0020441218020148